

Supporting Information

**Development of integrated microdroplet generation device with minimal loss for streamlining ddPCR-based SARS-CoV-2 detection**

Daekyeong Jung<sup>1,†</sup>, Hyowon Jang<sup>2,†</sup>, Jueun Kim<sup>3</sup>, Seok Jae Lee<sup>1</sup>, Nam Ho Bae<sup>1</sup>, Donggee Rho<sup>1</sup>, Bong Gill Choi<sup>3</sup>, Dae-Sik Lee,<sup>4</sup> Taejoon Kang<sup>\*2,5</sup>, and Kyoung G. Lee<sup>\*1</sup>

<sup>1</sup>Center for Nano Bio Development, National Nanofab Center, 291 Daehak-ro, Yuseong-gu, Daejeon 34141, Republic of Korea

<sup>2</sup>Bionanotechnology Research Center, Korea Research Institute of Bioscience and Biotechnology (KRIBB), 125 Gwahak-ro, Yuseong-gu, Daejeon 34141, Republic of Korea

<sup>3</sup>Department of Energy Resources and Chemical Engineering, Kangwon National University, 346 Jungang-ro, Samcheok, Gangwon-do 25913, Republic of Korea

<sup>4</sup>Department of Laboratory Medicine, Gyeongsang National University Hospital, Gyeongsang National University College of Medicine, 79 Gangnam-ro, Jinju, Gyeongsangnam-do 52727, Republic of Korea

<sup>5</sup>Welfare & Medical ICT Research Department, Electronics and Telecommunications Research Institute (ETRI), 218 Gajeong-ro, Yuseong-gu, Daejeon 34129 Republic of Korea

<sup>6</sup>School of Pharmacy, Sungkyunkwan University (SKKU), 2066 Seobu-ro, Jangan-gu, Suwon, Gyeonggi-do 16419, Republic of Korea

†These authors contributed equally to this work

\*E-mail: kglee@nnfc.re.kr (K.G.L.) and kangtaejoon@kribb.re.kr (T.J.)

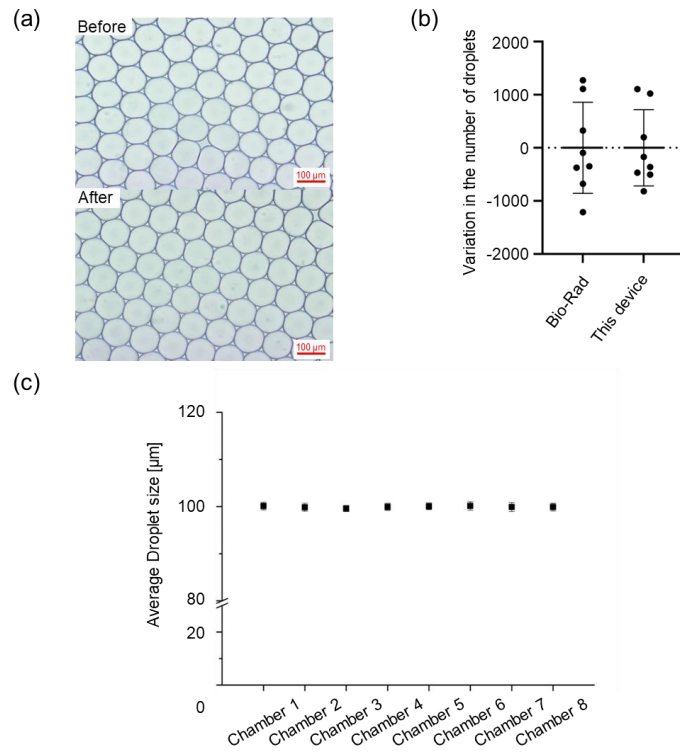


**Figure S1.** (a) Optical microscopy image of the droplets taken before and after PCR. (b) Plots of the variation in the number of microdroplets after the PCR for each instrument. Y-axis is the number of microdroplets deviating from the mean number of microdroplets. (c) Graph for the droplet size distribution of each chamber ( $n = 3$  independent experiments, error bar = standard deviation).

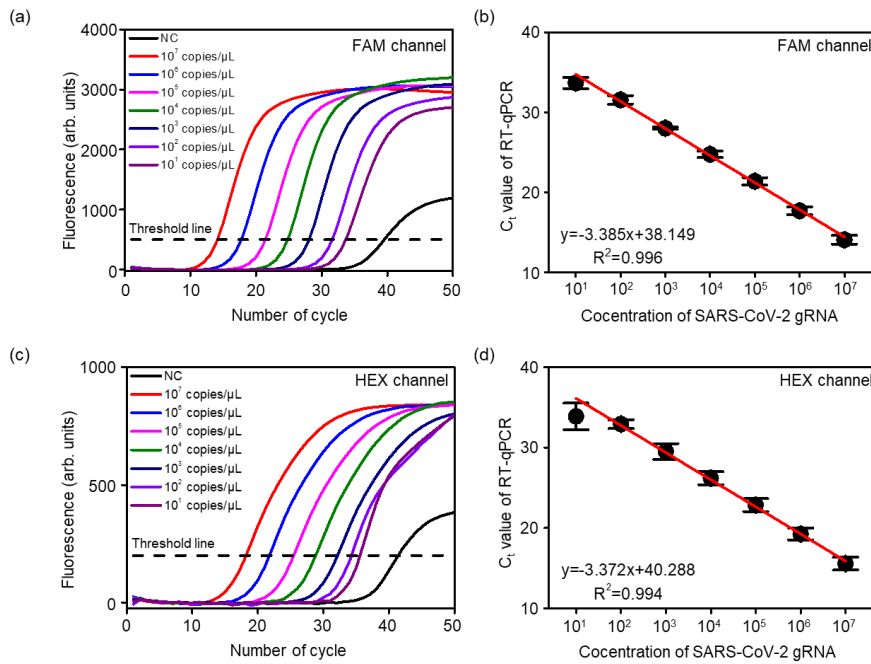


**Figure S2.** (a, c) Time-dependent fluorescence intensities during RT-qPCR with various concentrations of SARS-CoV-2 gRNA in (a) FAM and (c) HEX channel. (b, d) Correlation of  $C_t$  value to the logarithm of SARS-CoV-2 gRNA concentration in (b) FAM and (d) HEX channel. (n = 3 independent experiments, error bar = standard deviation). Red lines are linear fits. Dashed black threshold lines indicate the number of cycles at which the fluorescence intensity reached 500 in Figure S2a and 200 in Figure S2c (cycle threshold).

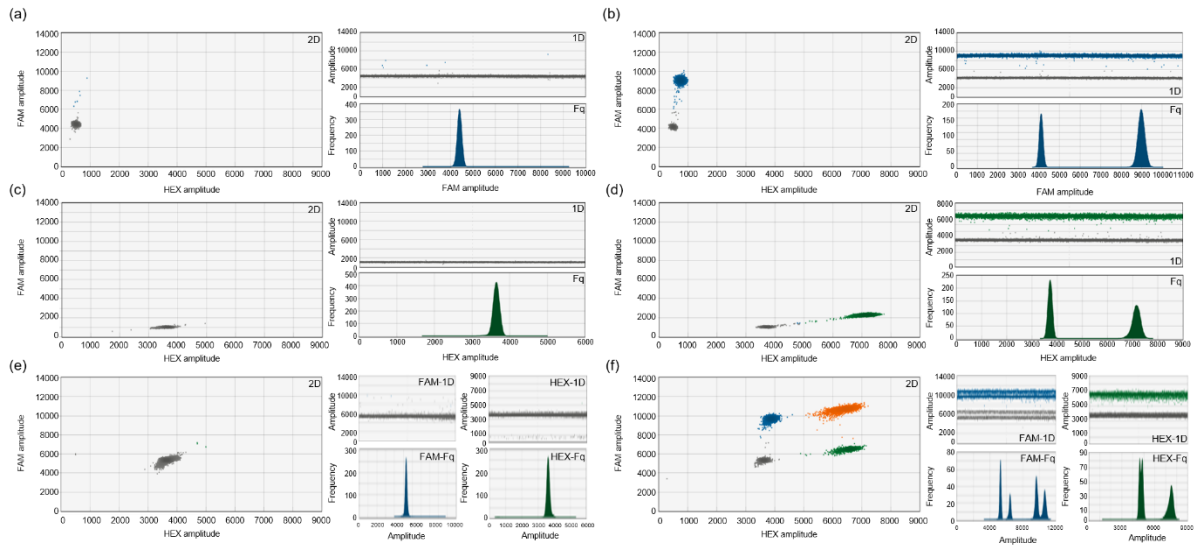


**Figure S3.** (a, b) ddPCR analysis result using only S gene specific primer/probe for (a) no template control and (b)  $10^5$  copies/ $\mu\text{L}$  of SARS-CoV-2 gRNA. (c, d) ddPCR analysis result using only E gene specific primer/probe for (c) no template control and (d)  $10^5$  copies/ $\mu\text{L}$  of SARS-CoV-2 gRNA. (e, f) ddPCR analysis result using both S and E gene specific primer/probe sets for (e) no template control and (f)  $10^5$  copies/ $\mu\text{L}$  of SARS-CoV-2 gRNA. 1D, 2D, and Fq indicates 1-dimensional amplitude analysis, 2-dimensional amplitude analysis, and frequency, respectively

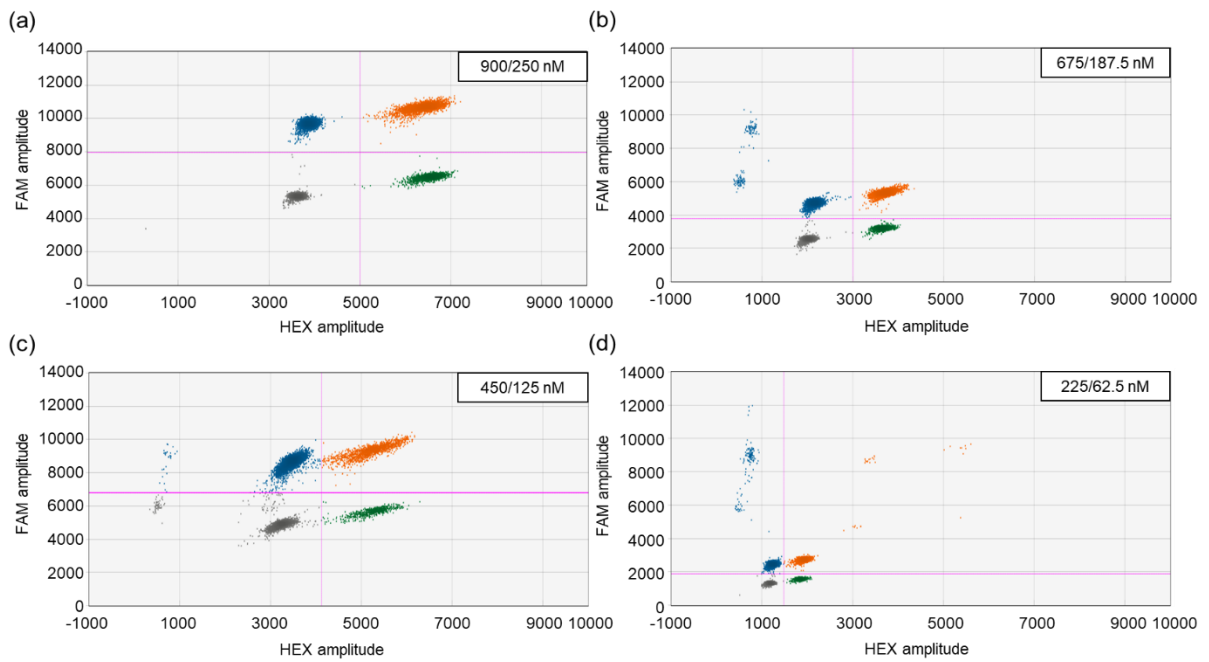


**Figure S4.** (a to d) 2D scatter plots of the ddPCR multiplex detection for the optimization of the primer/probe concentration. The primer and probe concentrations used are written in the top right of each image (a: 900/250 nM, b: 675/187.5 nM, c: 450/125 nM, d: 225/62.5 nM). The concentration of SARS-CoV-2 gRNA is  $10^5$  copies/ $\mu$ L.

**Table S1.** Sequence of oligonucleotides used in this study.

<b>Name</b>	<b>Sequence (5' -&gt; 3')</b>	<b>Target</b>
Forward primer	TGCTTTCGTGGTATTCTTGCT	E gene
Reverse primer	FAM – AGTTACACTAGCCATCCTTACTGC – BHQ1	
Taqman probe	AGTACGCACACAATCGAAGC	
Forward primer	TGCCTTGGTGATATTGCTGC	S gene
Reverse primer	SUN – TTGCCACCTTTGCTCACAGA – BHQ1	
Taqman probe	TACCCGCTAACAGTGCAGAA	

**Table S2.** RT-qPCR result of clinical samples.

<b>Patient number</b>	<b>C<sub>t</sub> (FAM)</b>	<b>C<sub>t</sub> (HEX)</b>
1	31.88155	32.95161
2	31.40239	32.63876
3	32.71348	33.58337
4	30.76304	31.86709
5	29.07234	30.11958
6	33.73801	33.85706
7	34.56252	32.87488
8	25.2015	26.22843
9	29.80289	30.77631
10	27.53214	28.59488
11	26.04448	27.08969
12	27.32305	28.44066
13	32.33148	33.51168
14	29.51884	29.89764
15	31.15536	32.2435
16	30.48291	31.41682
17	28.24187	29.32515
18	17.35145	18.42812
19	20.08618	21.17457
20	24.47696	25.68631
21	25.71989	26.8071
22	23.81248	24.95677
23	25.39568	26.52038
24	28.47631	29.44578
25	30.73636	31.86825
26	30.01407	31.31513
27	23.10092	23.97418
28	Not available	Not available
29	Not available	Not available
30	Not available	Not available
31	Not available	Not available

32	Not available	Not available
33	Not available	Not available
34	Not available	Not available
35	Not available	Not available
36	Not available	Not available
37	Not available	Not available
38	Not available	Not available
39	Not available	Not available
40	Not available	Not available
41	Not available	Not available
42	Not available	Not available
43	Not available	Not available
44	Not available	Not available
45	Not available	Not available



**Table S3.** RoC curve analysis result with respect to the Figure 4b.

Cut-off	Sensitivity%	95% CI	Specificity%	95% CI
> 0.5000	100	87.54% to 100.0%	5.556	0.2850% to 25.76%
> 0.8333	100	87.54% to 100.0%	16.67	5.837% to 39.22%
> 1.167	100	87.54% to 100.0%	22.22	9.001% to 45.21%
> 1.667	100	87.54% to 100.0%	33.33	16.28% to 56.25%
> 2.167	100	87.54% to 100.0%	44.44	24.56% to 66.28%
> 2.833	100	87.54% to 100.0%	55.56	33.72% to 75.44%
> 3.500	100	87.54% to 100.0%	61.11	38.62% to 79.69%
> 3.833	100	87.54% to 100.0%	72.22	49.13% to 87.50%
> 4.167	100	87.54% to 100.0%	83.33	60.78% to 94.16%
> 4.667	100	87.54% to 100.0%	88.89	67.20% to 98.03%
> 5.854	100	87.54% to 100.0%	94.44	74.24% to 99.72%
> 6.854	96.3	81.72% to 99.81%	94.44	74.24% to 99.72%
> 8.569	96.3	81.72% to 99.81%	100	82.41% to 100.0%
> 13.43	92.59	76.63% to 98.68%	100	82.41% to 100.0%
> 16.73	88.89	71.94% to 96.15%	100	82.41% to 100.0%
> 17.02	85.19	67.52% to 94.08%	100	82.41% to 100.0%
> 20.54	81.48	63.30% to 91.82%	100	82.41% to 100.0%
> 24.50	77.78	59.24% to 89.39%	100	82.41% to 100.0%
> 34.72	74.07	55.32% to 86.83%	100	82.41% to 100.0%
> 51.94	70.37	51.52% to 84.15%	100	82.41% to 100.0%
> 64.21	66.67	47.82% to 81.36%	100	82.41% to 100.0%
> 70.21	62.96	44.23% to 78.47%	100	82.41% to 100.0%
> 74.84	59.26	40.73% to 75.49%	100	82.41% to 100.0%
> 86.76	55.56	37.31% to 72.41%	100	82.41% to 100.0%
> 97.24	51.85	33.99% to 69.26%	100	82.41% to 100.0%
> 113.0	48.15	30.74% to 66.01%	100	82.41% to 100.0%
> 129.3	44.44	27.59% to 62.69%	100	82.41% to 100.0%
> 206.7	40.74	24.51% to 59.27%	100	82.41% to 100.0%
> 317.8	37.04	21.53% to 55.77%	100	82.41% to 100.0%
> 519.2	33.33	18.64% to 52.18%	100	82.41% to 100.0%
> 763.2	29.63	15.85% to 48.48%	100	82.41% to 100.0%
> 883.8	25.93	13.17% to 44.68%	100	82.41% to 100.0%
> 1011	22.22	10.61% to 40.76%	100	82.41% to 100.0%
> 1700	18.52	8.181% to 36.70%	100	82.41% to 100.0%
> 8913	14.81	5.916% to 32.48%	100	82.41% to 100.0%
> 16243	11.11	3.852% to 28.06%	100	82.41% to 100.0%
> 58482	7.407	1.316% to 23.37%	100	82.41% to 100.0%

**Table S4.** RoC curve analysis result with respect to the Figure 4d.

Cut-off	Sensitivity%	95% CI	Specificity%	95% CI
> 0.4167	100	87.54% to 100.0%	11.11	1.974% to 32.80%
> 0.5833	100	87.54% to 100.0%	16.67	5.837% to 39.22%
> 0.7500	100	87.54% to 100.0%	27.78	12.50% to 50.87%
> 0.9167	100	87.54% to 100.0%	33.33	16.28% to 56.25%
> 1.083	100	87.54% to 100.0%	38.89	20.31% to 61.38%
> 1.250	100	87.54% to 100.0%	44.44	24.56% to 66.28%
> 1.417	100	87.54% to 100.0%	50	29.03% to 70.97%
> 1.667	100	87.54% to 100.0%	55.56	33.72% to 75.44%
> 1.917	100	87.54% to 100.0%	61.11	38.62% to 79.69%
> 2.083	100	87.54% to 100.0%	66.67	43.75% to 83.72%
> 2.250	100	87.54% to 100.0%	72.22	49.13% to 87.50%
> 2.500	100	87.54% to 100.0%	77.78	54.79% to 91.00%
> 2.750	100	87.54% to 100.0%	83.33	60.78% to 94.16%
> 3.083	100	87.54% to 100.0%	88.89	67.20% to 98.03%
> 3.500	100	87.54% to 100.0%	94.44	74.24% to 99.72%
> 4.113	100	87.54% to 100.0%	100	82.41% to 100.0%
> 5.637	96.3	81.72% to 99.81%	100	82.41% to 100.0%
> 8.767	92.59	76.63% to 98.68%	100	82.41% to 100.0%
> 11.34	88.89	71.94% to 96.15%	100	82.41% to 100.0%
> 12.21	85.19	67.52% to 94.08%	100	82.41% to 100.0%
> 14.33	81.48	63.30% to 91.82%	100	82.41% to 100.0%
> 17.35	77.78	59.24% to 89.39%	100	82.41% to 100.0%
> 25.19	74.07	55.32% to 86.83%	100	82.41% to 100.0%
> 38.31	70.37	51.52% to 84.15%	100	82.41% to 100.0%
> 47.94	66.67	47.82% to 81.36%	100	82.41% to 100.0%
> 51.36	62.96	44.23% to 78.47%	100	82.41% to 100.0%
> 56.67	59.26	40.73% to 75.49%	100	82.41% to 100.0%
> 65.41	55.56	37.31% to 72.41%	100	82.41% to 100.0%
> 71.21	51.85	33.99% to 69.26%	100	82.41% to 100.0%
> 81.68	48.15	30.74% to 66.01%	100	82.41% to 100.0%
> 91.71	44.44	27.59% to 62.69%	100	82.41% to 100.0%
> 155.8	40.74	24.51% to 59.27%	100	82.41% to 100.0%
> 250.3	37.04	21.53% to 55.77%	100	82.41% to 100.0%
> 404.1	33.33	18.64% to 52.18%	100	82.41% to 100.0%
> 562.0	29.63	15.85% to 48.48%	100	82.41% to 100.0%
> 644.9	25.93	13.17% to 44.68%	100	82.41% to 100.0%
> 761.5	22.22	10.61% to 40.76%	100	82.41% to 100.0%

> 1295	18.52	8.181% to 36.70%	100	82.41% to 100.0%
> 7687	14.81	5.916% to 32.48%	100	82.41% to 100.0%
> 15281	11.11	3.852% to 28.06%	100	82.41% to 100.0%
> 35218	7.407	1.316% to 23.37%	100	82.41% to 100.0%
> 76744	3.704	0.1900% to 18.28%	100	82.41% to 100.0%